Time-lapse 3D CSEM for reservoir monitoring based on rock physics simulation

M. Ettayebi, S.Wang, M.Landrø [1]

[1]Norwegian University of Science and Technology (NTNU), mohammed.ettayebi@ntnu.no,
shunguo.wang@ntnu.no, martin.landro@ntnu.no

SUMMARY

Marine controlled-source electromagnetic (CSEM) method measures EM fields transmitted by an active source either at seafloor or a few tens of meters above the seafloor, therefore it can image the electrical resistivity beneath the seafloor. Being able to resolve resistivity anomalies of high saturations of petroleum, marine CSEM sounding has gained increasing popularity after its introduction in 1981 by Cox. Nevertheless, the EM research community starts to extend its applications from petroleum exploration to an active production monitoring tool. Our study focuses on the latter.

By utilizing various dynamic reservoir properties made available through reservoir simulation of the Wisting field located in the Norwegian part of the Barents Sea, a realistic geoelectric model was created. To this end, we develop geologically consistent rock physics models, such that the available simulation results can be transformed into resistivity maps. We show that the resistivity map pertaining to each time-step can be used as an input model in a Finite Difference Time Domain (FDTD) forward modeling workflow to produce synthetic EM data. This synthetic EM data can be studied and analyzed in light of production induced changes in the reservoir for different production phases. This will allow us to acquire insights towards developing a technically feasible reservoir monitoring workflow suitable for time-lapse CSEM. Our result shows that at different production phases, the CSEM responses are different. Therefore, the method can be effectively used for production monitoring purpose. Moreover, this study will enable the testing of other time-lapse workflows with realistic complexities evaluating the potential of this technology for field application, through investigating the resolution limitations and the repeatability requirements.

Keywords: CSEM, time-lapse, reservoir monitoring, production monitoring, 4D

INTRODUCTION

The controlled-source electromagnetic (CSEM) experiment has for decades been established as a reliable method for hydrocarbon exploration. It is also widely acknowledged as a complementary tool to the seismic experiment, mainly due to the high sensitivity of the method to resistive and conductive anomalies, such as oil reservoirs and water. Recently, several studies have been devoted to extending the applications of the CSEM method from merely being a risk-reduction tool to time-lapse production monitoring tool. However, there is a lack of research that thoroughly studies the potential of the CSEM tool in capturing production induced changes in the fluid content for realistic and detailed reservoir models and production strategies.

Currently, an increasing attention is drawn towards understanding the time-lapse behaviour of the CSEM method in detail. Therefore, we conduct research on how to enable time-lapse 3D CSEM for reservoir monitoring. By developing a geologically consistent rock-physics model, the dynamic reservoir properties of the Wisting field located in the Norwegian part of the Barents sea can be converted into resistivity models for each time-step. These resistivity models can be utilized as inputs in a Finite Difference Time Domain (FDTD) workflow to generate synthetic EM data that can be studied and analyzed for time-lapse production effects.

The Wisting discovery was made back in 2013 by the wildcat well 7324/8-1. The well was drilled down-flanks on a structure in the Wisting Central prospect and hence got the name central well (Fig-

ure 1). The reservoir at this area shows good quality, and it belongs to the Realgrunnen Subgroup which consists of three formations: Fruholmen, Nordmela and Stø Formations. The well entered the top of the reservoir which is the Stø Formation at the depth of 662 m. The water depth here is 400 m and the structural crest is currently at 250 m burial depth. Wisting is known for its discernible electric properties where the background resistivity can reach up to 20 Ωm (Granli et al, 2017). The central well (7324/8-1) was drilled with the primary objective of investigating and evaluating the Jurassic Realgrunnen Subgroup for hydrocarbons (NPD, 2022), which indeed ended up as a discovery well.
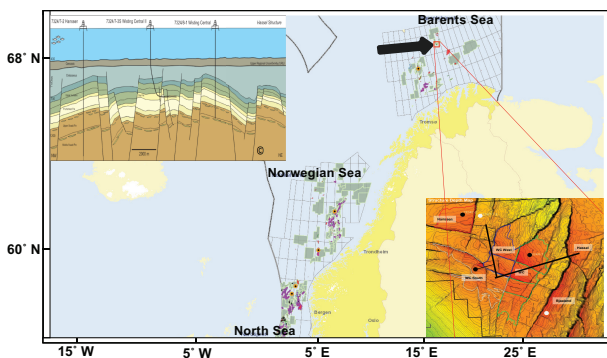

Figure 1: The Wisting field located in the Norwegian part of the Barents Sea as highlighted by the red rectangle. Lower right corner: the structure depth map of the Wisting field. The thick black lines are intersection lines going through specific wells. Upper left corner: schematic representation of the local structural and sedimentological geology along both of the thick black lines shown in the lower right corner.

A large database was made available for this time-lapse study, consisting of Eclipse production simulation models, well-logs, 3D CSEM inversion results and both conventional and P-cable 3D seismic data. The main objective of this work is to employ and combine the available data in various extents into a rock physics framework enabling us to create a serial of realistic resistivity models to represent oil production phases. These models can be utilized to investigate the survey parameters repeatability requirements and feasibility of time-lapse CSEM. With that in mind, this study consists of two main parts. The first one deals with the construction and calibration of the reservoir model while the second is devoted to studying the feasibility of time-lapse CSEM. As for the repeatability requirements, we will investi-

gate that in future research.

RESISTIVITY MODELING FROM TIME-VARYING WATER SATURATION SIMULATIONS

CSEM data can be used to image resistivity structures. Subsequently, getting insight into the different rock properties that can alter subsurface resistivity is of critical importance for CSEM interpretation. Therefore, creating a reservoir model that will be used for time-lapse CSEM does depend on the resistivity distribution across the field considered. This brings into question the importance of a precise and realistic mapping of the resistivity. Time-varying water saturation can be transformed to time-varying resistivities and subsequently to time-varying Anomalous Transverse Resistance (ATR) maps. The Wisting field has demonstrated an excellent oppurtunity to show the ability of CSEM for reservoir monitoring.

The reservoir resistivity is dependent on a number of subsurface parameters. By Archie's law (Archie, 1942) it is clear that the saturation exponent n is one important parameter. Archie's law makes three implicit assumptions as pointed out by Mungan and Moore (1968); one is that the only conductive material is brine and that the rock matrix is non-conductive. However, if the reservoir contains clay, then rather more advanced models are required to model it.

Another physical property that has close interplay with reservoir resistivity is rock wettability and its distribution. Mungan and Moore (1968) state that the saturation exponent n appears to be saturation dependent increasing with the decrease of water saturation, and it can be as high as 9 when the water saturation is approaching connate water saturation in oil-wet formations. Bearing in mind that the reservoir at Wisting is possibly oil-wet as suggested by Alvarez et al (2018), this introduces the possibility of adjusting the saturation exponent n resulting in higher modeled resistivities.

As previously studied, there are many factors that can alter the saturation exponent and one of these factors is wettability (Adisoemarta et al, 2001). The model developed here and which is calibrated with the central well, elaborates further on this in conjunction with the conclusions made by Mungan and Moore (1968) on oil-wet formations. The model deals with the non-linearity of the saturation expo-

nent in oil-wet formations depending on water saturation. The saturation exponent should increase significantly in oil-wet formations to account for the isolated water globules in the larger pores, and which will not be able to conduct current (Anderson, 1986). Moreover, the wettability effects become more prominent as the brine saturation decreases. This stipulates establishing a connate water saturation $S_{w,connate}$ threshold or cut-off below which the rock changes its wettability from a state of mixed wettability to becoming oil-wet, resulting in a larger saturation exponent. The fact that Alvarez et al (2018) use a saturation exponent equal to 2.8 in their Wisting resistivity modeling supports the claim of Wisting being oil-wet. By incorporating information from both capillary pressure curves and Free Water Level (FWL) depth maps, the connate water saturation threshold was set to 10%.

Different gas caps scattered over the field have been recognized and these deserve special treatment in terms of the saturation exponent n. The latter should most likely be less than 2 in gas-bearing formations, introducing the necessity for choosing another threshold value for the gas saturation which for the reader's convenience will be given the name critical gas saturation. This may consequently demarcate the transition from oil-wet rocks with low water saturation combined with a large saturation exponent on one hand, and gas-bearing zones with relatively high gas saturation combined with a lower saturation exponent on the other hand. After multiple attempts, a gas saturation threshold value equal to 70% was deemed to produce the desired models. By desired models, the generated ATR maps are consistent with our understanding of the spatial distribution and magnitude of the most resistive targets and this conforms with the inverted 3D CSEM ATR maps.

With this background, a non-linear saturation exponent was modeled having its maximum value of 2.5 at the top of the reservoir and non-linearly decreasing with depth and the overall water saturation trend. Note that this only applies for intervals where the water saturation is lower than the connate water saturation 10%. On the other hand, if the gas saturation is higher than the critical gas saturation, then the saturation exponent n is assigned the value 1.8. To summarize, there are two main factors that decide what kind of value the saturation exponent is assigned, and these are the connate water saturation and critical gas saturation thresholds. The rock-physics model was used to transform detailed water saturation simulations to detailed resistivity maps that are used as inputs in a FDTD forward modeling

workflow to generate synthetic CSEM data. Two resistivity maps are presented in Figure 2, in which the reservoir is marked by warm color.
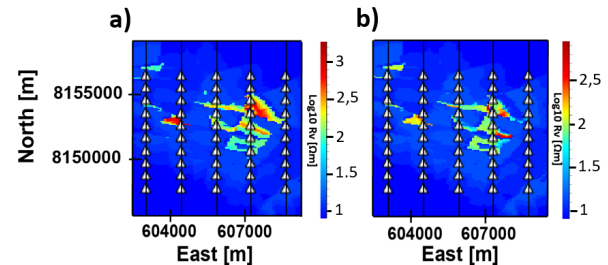

Figure 2: 2D resistivity maps for two different time steps. The year 2027 (plot a) when the field is expected to start producing and in the year 2057 (plot b) towards the predicted end of production. The white rectangles are receivers and the black vertical lines going through them are towlines. Note that the colorbar scales pertaining to the two different plots are different.

TIME-LAPSE PRODUCTION INDUCED RESPONSES

The time steps at the onset of production in the year 2027 and after 30 years of production in the year 2057 are used for simulation. Figure 3 shows the Ex-field normalized magnitude (NM) maps pertaining to the last time step. The source-receiver offset is set to 2667 m and the frequency is 5.0 Hz. Normalized value 1 represented by the lightish green implies that no change happens through the 30 years. If the NM is larger than 1, one can assume that there are changes to spot in the fluid content of the subsurface reservoir. It is clear that Figure 3 depicts discernible production-induced changes represented by the red positive anomalies. A clear and good spatial match exists between these anomalies and the resistivity maps in Figure 2, as we can clearly see that the epicentre of the anomaly is where most of the production is predicted to take place. A producing hydrocarbon field is expected to have decreasing petroleum volumes with time and hence lower resistivity values due to water-injection. Towards the end of the lifetime of a producing field, most of the target resistor will be gone and the end result is without the target resistor embedded in it. Figure 3 underpins this fact with the positive anomaly, which implies that the target response in the year 2027 is larger than the pseudo-background response in the year 2057. Another observation worth mentioning is the relatively

high frequency depicted here, and the higher resolution that offers. We think that a combination of relatively high background resistivity and shallow burial depth might contribute to a setting that is favorable for slightly higher frequencies.
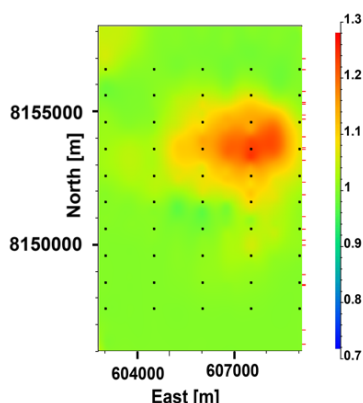

Figure 3: Normalized magnitude (NM) 2D map of the E_x field component for the year 2057 towards the predicted end of production. The source-receiver offset is 2667m while the frequency is 5.0 Hz. The black dots are receiver positions.

CONCLUSION

We showed how dynamic reservoir simulations related to different time steps can be converted to resistivity spatial distributions through a detailed, realistic and geologically consistent rock-physics model. These resistivity maps can be used as inputs in a FDTD forward modeling workflow to generate synthetic CSEM data. The CSEM data are studied and analyzed in different approaches towards understanding and developing a feasible workflow for time-lapse CSEM studies. What comes forth through this study is the ability of CSEM data to detect and capture production induced changes in the fluid content of a producing hydrocarbon reservoir. In addition, the presented workflow proves itself to be a feasible one, demonstrating how time-lapse CSEM can be used. The future work is to take a closer look at the repeatability requirements and limitations of time-lapse marine CSEM.

ACKNOWLEDGMENTS

REFERENCES

Adisoemarta PS, Anderson GA, Frailey SM, Asquith GB (2001) Saturation exponent n in well log interpretation: Another look at the permissible range. SPE Permian Basin Oil and Gas Recovery Conference DOI 10.2118/70043-ms

Alvarez P, Marcy F, Vrijlandt M, Skinnemoen Ø, MacGregor L, Nichols K, Keirstead R, Bolivar F, Bouchrara S, Smith M, Tseng HW, Rappke J (2018) Multiphysics characterization of reservoir prospects in the hoop area of the barents sea. Interpretation 6(3):SG1–SG17, DOI 10.1190/int-2017-0178.1

Anderson WG (1986) Wettability literature survey-part 3: The effects of wettability on the electrical properties of porous media. Journal of Petroleum Technology 38(12):1371–1378, DOI 10.2118/13934-pa

Archie G (1942) The electrical resistivity log as an aid in determining some reservoir characteristics. Transactions of the AIME 146(01):54–62

Granli JR, Veire HH, Gabrielsen P, Morten JP (2017) Maturing broadband 3D CSEM for improved reservoir property prediction in the Realgrunnen Group at Wisting, Barents Sea. SEG Technical Program Expanded Abstracts 2017 pp 2205–2209

Mungan N, Moore E (1968) Certain wettability effects on electrical resistivity in porous media. Journal of Canadian Petroleum Technology 7(01):20–25, DOI 10.2118/68-01-04

NPD F (2022) 7324/8-1 general information. https://factpages.npd.no/en/wellbore/pageview/exploration/all/7 accessed: 2022-06-11